Hindawi Publishing Corporation
International Journal of Photoenergy
Volume 2014, Article ID 490264, 11 pages
http://dx.doi.org/10.1155/2014/490264

Research Article

Effect of Isopropanol on Microstructure and Activity of TiO_2 Films with Dominant {001} Facets for Photocatalytic Degradation of Bezafibrate

Murtaza Sayed,[1,2] Fu Pingfeng,[3] Hasan M. Khan,[2] and Pengyi Zhang[1]

[1] *State Key Joint Laboratory of Environment Simulation and Pollution Control, School of Environment, Tsinghua University, Beijing 100084, China*
[2] *Radiation Chemistry Laboratory, National Centre of Excellence in Physical Chemistry, University of Peshawar, Peshawar 25120, Pakistan*
[3] *School of Civil and Environment Engineering, University of Science and Technology Beijing, Beijing 100083, China*

Correspondence should be addressed to Pengyi Zhang; zpy@tsinghua.edu.cn

Received 17 February 2014; Accepted 14 May 2014; Published 11 June 2014

Academic Editor: Jimmy C. Yu

Titanium dioxide (TiO_2) films with dominant {001} facets coated on a titanium sheet (Ti) were synthesized with the simple hydrothermal method by using Ti as the precursor and substrate. The effect of addition of isopropanol into the hydrothermal solution on the structure, photocatalytic activity, and stability of as-synthesized TiO_2 films was investigated. The presence of isopropanol obviously influenced the microstructure of as-synthesized TiO_2 films, which was converted from microspheres into irregular close stack of truncated tetrahedrons. And the percentage of exposed {001} facets calculated from the Raman spectra increased from 48.2% to 57%. Accordingly, the TiO_2 films prepared with addition of isopropanol showed high and stable photocatalytic activity, which is nearly 2.6 times as that of the conventional P25 TiO_2 coated on Ti-substrate. In addition, the photocatalytic activity of as-synthesized TiO_2 films was greatly enhanced after calcination treatment at 600°C, which can be attributed to removal of fluoride ions and organic residuals adsorbed on the surface of the catalyst. Photoluminescence (PL) technique was used for the detection of produced hydroxyl radicals ($^{\bullet}OH$) on the surface of UV-illuminated TiO_2 using terephthalic acid as probe molecule. The photocatalytic degradation intermediates of bezafibrate were analyzed by an ultraperformance liquid chromatography-tandem mass spectrometry (UPLC-MS/MS), and accordingly the degradation pathways were proposed.

1. Introduction

Semiconductor-based photocatalysis has found increasing interest to solve global environmental problems and has been proven to effectively degrade a great number of organic pollutants. Among them, TiO_2 is one of the most promising materials so far, because it is highly photoreactive, cheap, nontoxic, chemically and biologically inert, and photostable [1]. Due to the relatively high density of unsaturated 5-fold Ti-atoms and the unique electronic structure, {001} facets of anatase TiO_2possess higher photocatalytic activity over thermodynamic stable {101} facets [2–10]. Yang et al. [7] for the first time synthesized single-crystalline anatase with 47% exposed {001} facets through hydrothermally heating a mixed aqueous solution of $TiF_4$and HF, where the selective adsorption of fluoride ions stabilized the high-energy {001} facets. The exposed percentage of {001} facets was later increased to 64% and the as-synthesized anatase crystals were reported to generate much more hydroxyl radicals ($^{\bullet}OH$) upon UV irradiation than the commercial Degussa P25 [6]. Till now a lot of work has been conducted to increase the percentage of exposed {001} facets [2–4, 10–16].

In addition to the {001} facets TiO_2in the powder form, the immobilized films with exposed {001} facets were also reported in order to minimize the cost of separating powders from water after treatment and thus to make the process easy for practical applications. Wang et al. [17] for the first time fabricated the TiO_2-film with exposed {001} facets by

hydrothermal treatment of Ti-foil at 140°C in 40 mL of 0.01 M HF aqueous solution in a 80 mL Teflon lined stainless steel autoclave for 10 h. Zhang et al. [18] synthesized {001} facets TiO_2 crystals on titanium foil by hydrothermal treatment of titanium foil in a 60 mL of 0.5% (v/v) HF solution at 180°C for 3 h. Wu and Tang [19] fabricated {001} exposed TiO_2 film by immersing Ti-plate in a Teflon-lined autoclave for 1 to 24 h at 180°C. However to the best of our knowledge, there is little research on the role of isopropanol or other alcohols on the fabrication and photocatalytic stability of {001} facets exposed TiO_2 films immobilized on Ti-substrate. In this study, we found the presence of isopropanol in the hydrothermal solution makes {001} facets exposed TiO_2 films have sheet-like morphology, which possess higher activity and stability towards removal of organic contaminants as compared to TiO_2 microspheres with exposure of {001} facets.

Recently, pharmaceuticals and personal care products (PPCPS) have drawn increasing attention due to their pres ence in waters or soils [20]. Bezafibrate, that is, 2-(4-{2-[(4-chlorobenzoyl)amino]ethyl}phenoxy)-2-methylpropanoic acid, is a widely used lipid regulator drug throughout the world, and consequently it has been frequently detected in the environment [21, 22]. For example, in Germany this drug has been found in sewage treatment plants at a concentration of ~4.6 $\mu g\,L^{-1}$ [21, 22]. In rivers and water streams, its concentration is nearly 0.35 $\mu g\,L^{-1}$ [22]. In Italian rivers it has been found that bezafibrate concentration is ~57.15 $ng\,L^{-1}$ [23]. In surface waters, this drug has been detected at median concentrations of ~3.1 $\mu g\,L^{-1}$ [21]. The removal of bezafibrate has been investigated using different advanced oxidation processes (AOPs) such as photo-Fenton [24], photodegradation using solar-simulated irradiation [25], ozonation, and UV/H_2O_2 [26]; however no studies have been reported for the photocatalytic removal of bezafibrate by using TiO_2films with dominant {001} facets.

2. Experimental Section

2.1. Synthesis of TiO_2 Films with Dominant {001} Facets. Ti-sheet (99.5% in purity, Baoji Shengrong Titanium Corporation, China), with a size of 180 mm × 120 mm × 0.15 mm, was first pretreated in an oxalic acid solution for 40 min at 100°C. The pretreated Ti-foil was then hydrothermally treated at 180°C in aqueous solution of 0.03 M HF in a Teflon-lined autoclave with a total capacity of 160 mL. To study the role of isopropanol on the stability and formation of {001} facets, two different ratios of isopropanol were tried, that is, 0 and 50 mL, keeping all the other experimental conditions the same. After hydrothermal treatment, the obtained Ti-sheets with {001} facets were washed with distilled water for 3 times and then dried in air at room temperature. Finally, the Ti-sheets with {001} facets were calcined in air at 600°C for 90 min. For simplicity we named the two samples as S0 (without isopropanol) and S1 (with isopropanol).

2.2. Characterization. The morphology of as-synthesized TiO_2 film was observed with an ultrahigh resolution field-emission scanning electron microscope (FESEM, S-5500, Hitachi) performed at an accelerating voltage of 5.0 kV. The high resolution transmission electron microscopy (HRTEM) analysis was conducted using a JEM-2011F electron microscope (JEOL, Japan). To prepare the TEM specimen, the TiO_2 films on the Ti-sheet were first ultrasonically peeled in absolute ethanol for 40 min and then the suspension was dropped on carbon film supported on copper grid and dried in air before analysis. X-ray diffraction (XRD) analysis was carried out with a Rigaku D/max-RB using Cu Kα radiation (λ = 0.15418 nm), operated at 40 kV and 100 mA. Chemical states of surface elements were investigated by X-ray photoelectron spectroscopy (XPS, PHI-5300, ESCA) at a pass energy of 50 eV, using Al Kα as an exciting X-ray source. Raman spectra were recorded on an inVia Raman microscope (Renishaw) at the range of 100–800 cm^{-1}. The diffuse reflectance absorption spectra (DRS) of the samples were recorded on a UV-Vis spectrophotometer (Hitachi UV-3010) by using $BaSO_4$ as the reference standard.

2.3. Photocatalytic Procedures. Photocatalytic activity was measured by taking 10 mg/L of bezafibrate (Sigma-Aldrich) solution in a 120 mL cylindrical vessel into which TiO_2/Ti-sheet with dominant {001} facets was inserted. A 10 W low-pressure mercury lamp (λ_{max} = 254 nm) was used as the irradiation source. Oxygen gas was supplied from the bottom of the reactor at the flow rate of 30 mL/min. Aliquots were taken out every 15 min and the concentration of bezafibrate was determined with a high performance liquid chromatography (HPLC, Shimadzu, LC-10AD) with a UV detector (SPD-10AV) at 230 nm and a Kromasil C18 column (250 mm × 4.6 mm) for separation. The mobile phase was a mixture of methanol and water (70 : 30, v/v) at a flow rate of 1 mL min^{-1}. TiO_2(Degussa P25) was coated on Ti-sheet by dipping the Ti-sheet 15 times in TiO_2 aqueous suspension (10 g/L) and then calcining at 400°C for 90 min. P25 coated Ti-sheet was adopted as the reference with which the photocatalytic activity under the same experimental conditions is compared.

To check the stability of as-synthesized TiO_2 films (after calcination at 600°C), the photocatalytic activity of S0 and S1 samples to degrade bezafibrate was continuously tested for 6 times, and each test lasted for 120 min.

Degradation intermediates of bezafibrate were identified by an ultraperformance liquid chromatography-tandem mass spectrometry (UPLC-MS/MS). The optimized mass parameters were as follows: capillary voltage, 2.1 kV; source temperature, 120°C; desolvation temperature, 280°C; and desolvation gas flow rate, 650 L/h. The parent ion, daughter ion, cone voltage (V), and collision energy (eV) for bezafibrate detection were 360.22 > 274.12, 22, and 15. In addition, the full scan mode was used to detect parent ions for acquiring more information about intermediates. Samples were directly injected into the mass spectrometer ion source by pure methanol with the cone voltage of 10 V.

2.4. Detection of Hydroxyl Radicals. The production of hydroxyl radical ($^{\bullet}OH$) on the surface of UV-irradiated {001} facets TiO_2/Ti film was analyzed by photoluminescence technique (PL) using terephthalic acid as probe molecule.

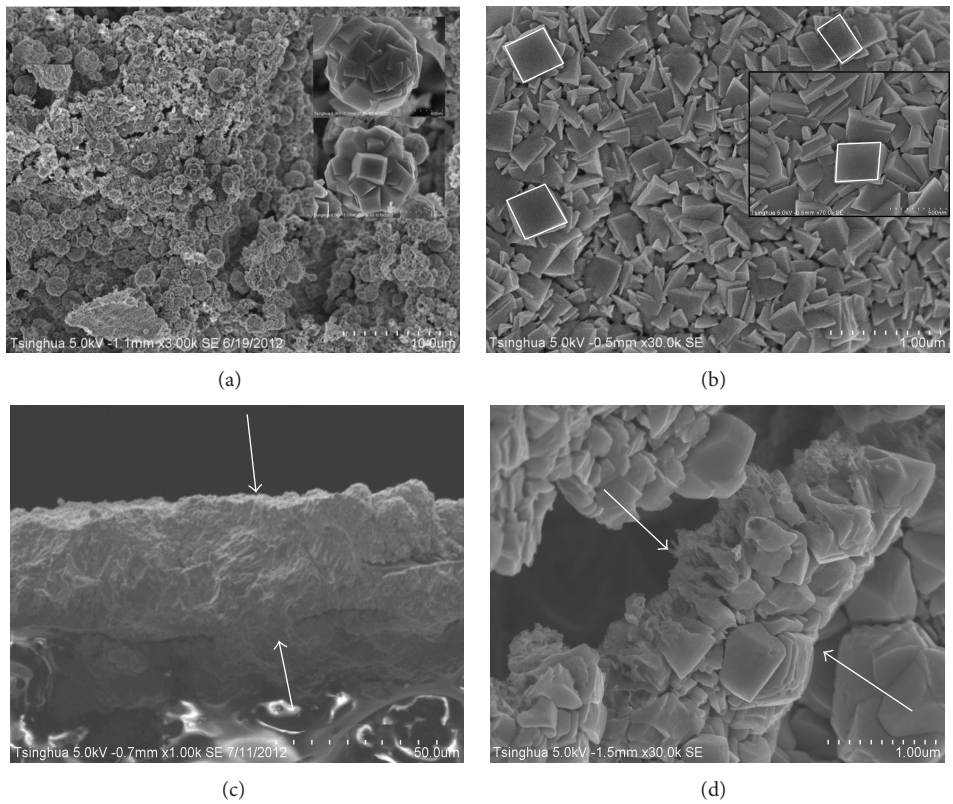

Figure 1: FE-SEM images of Ti-sheet treated in 0.03 M HF at 180°C for 3 h. (a) Without isopropanol, that is, S0, (b) with isopropanol, that is, S1, (c) cross-sectional view of S0, and (d) cross-sectional view of S1.

The reaction of terephthalic acid with produced $^{\bullet}$OH by means of UV-irradiation on the surface of {001} facets TiO_2/Ti films gives the formation of a fluorescent product 2-hydroxyterphthalic acid, whose PL intensity is in proportion to the formation of $^{\bullet}$OH in water [27]. In this method a small sheet (2.5 cm × 1 cm) of our as-synthesized film was placed in a mixed aqueous solution of 2×10^{-4} M terephthalic acid and 2×10^{-3} M NaOH under the UV-irradiation of a 15 W 254 nm lamp. Then after every 15 mins of UV-irradiation, the PL spectrum of produced 2-hydroxy terephthalic acid was taken on Hitachi F-7000 fluorescence spectrophotometer.

3. Results and Discussion

3.1. Morphology and Phase Structures. Figure 1 shows surface morphologies of samples S0 and S1. Truncated tetrahedrons with exposure of {001} facets can be clearly observed on the as-synthesized TiO_2 films. As shown in Figure 1(a), when no isopropanol was added in the hydrothermal solution, the TiO_2films generally consisted of microspheres assembled with nanosheets, which is in agreement with the literatures [4, 28]. However, in the case of isopropanol addition, the TiO_2 films almost consisted of irregular stack of truncated tetrahedrons without formation of microspheres (Figure 1(b)). Based on geometrical symmetry of anatase TiO_2, the top and lateral surfaces are {001} and {101} facets, respectively. These results demonstrate that while keeping other hydrothermal conditions the same, the microstructure of TiO_2 film can be affected by addition of isopropanol into the hydrothermal mixture. Figures 1(c) and 1(d) show the cross-sectional SEM images of samples S0 and S1. The film thickness was ~ 30 μm without addition of isopropanol, while it was reduced to ~0.8 μm when isopropanol was added to hydrothermal solution.

Generally the surface of TiO_2 in aqueous media exists in one of the possible species, that is, $TiOH_2^+$, TiO^-, or TiOH depending on the pH values [29]. In the solution of 0.03 M HF with pH 2.3, nearly 94.8% of previously dominated TiOH would be replaced by TiF through ligand exchange between surface hydroxyl (–OH) groups on TiO_2 and fluoride ions (F^-) in the aqueous solution, as illustrated by

$$\equiv\text{Ti–OH} + F^- \longrightarrow \equiv\text{Ti–F} + OH^- \quad (1)$$

It is well known that HF acts as a capping agent for the synthesis of anatase TiO_2 single crystal with {001} facets. In the presence of isopropanol along with HF, the isopropoxy ions (iPrO$^-$, $(CH_3)_2CHO^-$) will bind partially to Ti-atoms on the surface and accordingly more stable {001} facets are formed. Similar results were also reported by Yang et al. [6] where they synthesized single-crystal nanosheets with dominant {001} facets with a solvothermal method by using titanium tetrafluoride (TiF_4) as a precursor.

Solvents usually influence the growth and morphology of metal crystals due to difference in the viscosities of various

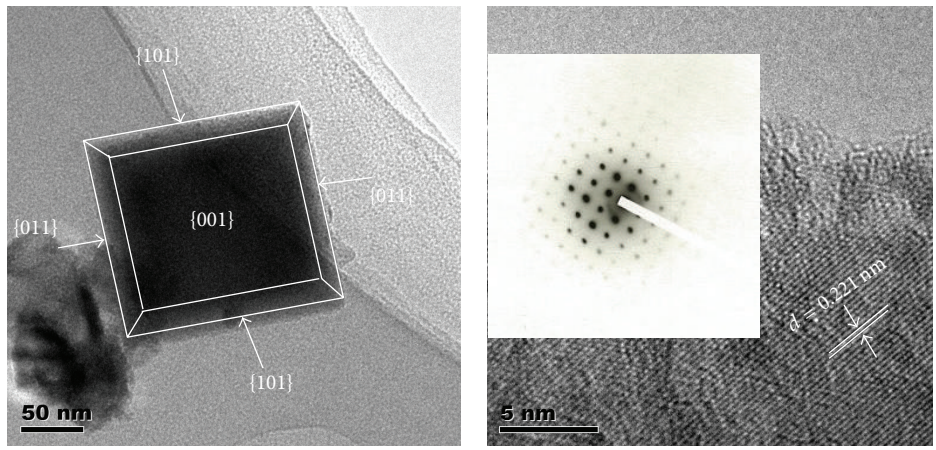

(a) (b)

FIGURE 2: (a) TEM image of single crystal anatase TiO_2 scratched from Ti-substrate of sample S1; (b) HR-TEM image of anatase TiO_2 single crystal recorded along {001} axis; the inset shows SAED pattern.

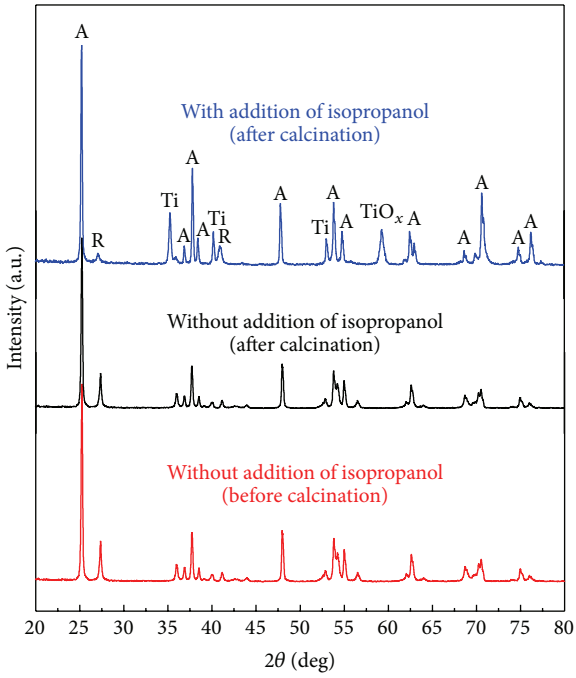

A: anatase
R: rutile
Ti: titanium

FIGURE 3: XRD patterns of the TiO_2 film synthesized with addition of isopropanol (before and after calcination treatment) and without addition of isopropanol.

solvents [30]. The present results show that an addition of isopropanol provided a good environment to strengthen the stabilization effects associated with fluorine adsorption on the {001} surface and thus enhanced its preferred growth and maximized the exposure of {001} facets. Figure 2(a) shows the high resolution transmission electron microscopy (HR-TEM) image of sample S1. The large square surface of the nanosheets is the {001} crystal facet and the small isosceles trapezoidal surfaces correspond to {101} crystal facet. Figure 2(b) shows the lattice spacing of 0.221 nm, which corresponds to (001) atomic planes of anatase TiO_2 and thus confirms the formation of {001} facets TiO_2. Selected area electron diffraction (SAED) pattern in the inset of Figure 2(b) confirms the single crystal nature of this TiO_2 particle and thus favors the migration of photogenerated electron-hole pairs [31, 32].

The XRD patterns of samples S0 and S1 are shown in Figure 3. It is clear that the diffraction peaks at $2\theta = 25.22^\circ$, 36.82°, 37.67°, 38.54°, 47.94°, 53.79°, 55.02°, 62.64°, 68.72°, and 70.51° can be attributed to (101), (103), (004), (112), (200), (105), (211), (213), (204), and (110) of the standard card JCPDS 21-1272 corresponding to anatase, suggesting a high phase purity for the achieved titania. It is also clear from our XRD patterns before and after calcination treatment that there was no change in crystal structure after heat treatment at 600°C. The synthesized TiO_2 films consist of ca. 83% anatase and 17% rutile. Besides TiO_2, there are other diffraction peaks at $2\theta = 35.96^\circ$, 39.95°, and 52.92° which correspond to titanium (Ti) sheet (JCPDS number 05-0628). There is also a diffraction peak at $2\theta = 53.82^\circ$ for sample S1 which belongs to TiO_x. The appearance of Ti diffraction peaks in XRD of the TiO_2 films grown on Ti-substrate was also reported by Wang et al. and Alivov and Fan [9, 17], respectively. The rutile character may be due to the Ti-substrate to which the TiO_2 film was directly attached [17].

3.2. Raman Spectra Analysis of {001} Facets TiO_2 Films. Raman spectroscopy was used for surface characterization and accordingly the percentage of exposed {001} facets for samples S0 and S1 was calculated. Figure 4 shows that all the samples were of similar peaks appearing at 145.8, 191 cm^{-1}, 399, 520, and 634 cm^{-1} indicating the anatase TiO_2 phase

[33, 34]. It can be noticed that as the percentage exposure of {001} facets increases, the intensity of E_g peak at 634 cm^{-1} reduced gradually, while the intensity of B_{1g} peak at 399 cm^{-1} and A_{1g} peak at 520 cm^{-1} increased simultaneously. It is well known that E_g peak mainly originates from stretching vibration of O–Ti–O in TiO_2, the B_{1g} peak is caused by symmetric bending vibration of O–Ti–O, and A_{1g} peak is mainly due to antisymmetric bending vibration of O–Ti–O [33]. The higher the percentage of exposed {001} facets, the less the number of stretching vibration modes of O–Ti–O, and consequently the intensity of E_g peak in the Raman spectra becomes decreased. On the other hand, when the exposed {001} facets become lowered, the number of symmetric bending vibrations and the antisymmetric bending vibrations of O–Ti–O increases. In the same way the higher the percentage of exposed {001} facets is, the more the number of symmetric bending vibrations and the antisymmetric bending vibrations of O–Ti–O will be, accordingly, and the intensity of A_{1g} and B_{1g} peaks in the Raman spectra becomes increased.

Based on the ratio of peak intensity of E_g at 145.8 cm^{-1} and peak intensity of A_{1g} at 511.7 cm^{-1} the percentage of exposed {001} facets in samples S0 and S1 was calculated to be 48.2% and 57.0%, respectively, according to a well-established method reported by Tian et al. [33].

Furthermore, the appearance of five active Raman modes confirms the formation of anatase TiO_2 film and supports our previous statement that the rutile character in our XRD may be due to Ti-substrate on which the TiO_2 film is grown [17]. On the basis of different detecting depths of XRD and Raman techniques, it can be suggested that the synthesized TiO_2 films may have layered structure, that is, Ti-foil, TiO_x, rutile TiO_2, and anatase TiO_2 with oriented {001} facets [17]. Besides, slight shifting of E_g peaks (145.8 cm^{-1} and 634 cm^{-1}) towards lower wave number was also observed for samples S0 and S1 which may be due to changes in the thickness of TiO_2 films or the increased particle size of TiO_2 films [35, 36].

3.3. XPS Analysis. To investigate the surface environment of as-synthesized {001} facets TiO_2 films, XPS spectrum survey was carried out for sample S1. As shown in Figure 5, before calcination treatment at 600°C, sharp photoelectron peaks appear at the binding energies (BE) 459.1 (Ti $2p_{3/2}$), 464.9 (Ti $2p_{1/2}$), 530.9 (O1s), 684.5 (F 1s), and 284.7 (C 1s) eV. The BE of Ti $2p_{3/2}$ and Ti $2p_{1/2}$ is slightly higher than the earlier reported values in fluorine terminated anatase TiO_2-sheet powder [7]. The F 1s peak at 684.5 eV is a typical value for the fluorinated TiO_2, and no signal of fluorine in the lattice of TiO_2 (688.5 eV) is observed [6, 27, 37]. As reported in literature [7], surface-bonded fluoride ions can be easily removed via being calcined at 600°C without affecting the crystal structure or morphology. It is confirmed in the present work that, as shown in Figure 5, F 1s peak at 684.5 eV was completely ruled out from as-synthesized {001} facets TiO_2 film after calcination treatment at 600°C.

3.4. Hydroxyl Radical Analysis. Figure 6 shows the PL spectra from terephthalic acid solution excited at 315 nm at different

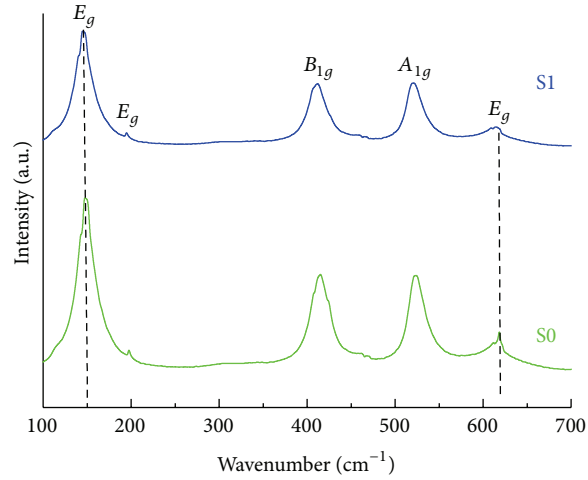

Figure 4: Raman Spectra of TiO_2 films synthesized with (S1) and without (S0) addition of isopropanol.

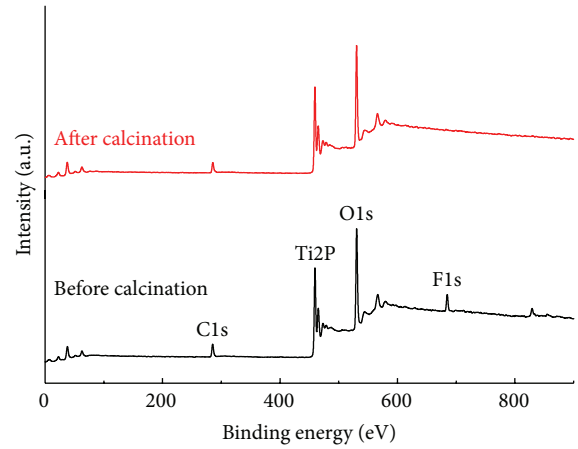

Figure 5: XPS spectra of TiO_2 film synthesized with addition of isopropanol before and after calcination.

UV-irradiation times. It can be seen that a gradual increase in PL intensity is observed at 425 nm with increase in UV-irradiation times. When there was no UV-irradiation supplied to the terephthalic acid sample solution, then no PL peak was observed, which means that fluorescence is only caused by product (2-hydroxyterephtahlic acid) formed by the reaction of terephthalic acid with $^{\bullet}OH$ radical. The PL results also suggest that $^{\bullet}OH$ radicals are produced on the surface of {001} facets TiO_2/Ti films when exposed to UV-irradiation.

3.5. Photocatalytic Activity and Stability. The photocatalytic activity of as-synthesized {001} facets TiO_2 films was examined by decomposing a pharmaceutical pollutant, that is, bezafibrate. Figure 7(a) shows the comparison of removal ratios of bezafibrate within 120 min by P25 TiO_2 films and {001} facets TiO_2 samples S0 and S1 before and after calcination treatment. All as-synthesized samples whether they

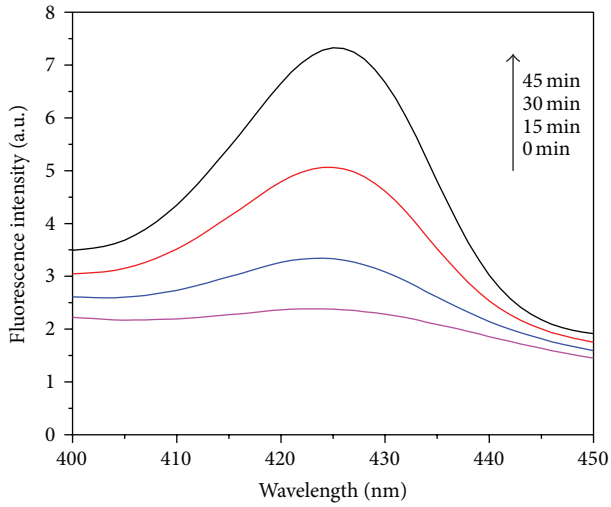

Figure 6: PL spectral changes observed during UV-illuminated {001} facets TiO_2/Ti film in mixed solution of terephthalic acid and NaOH.

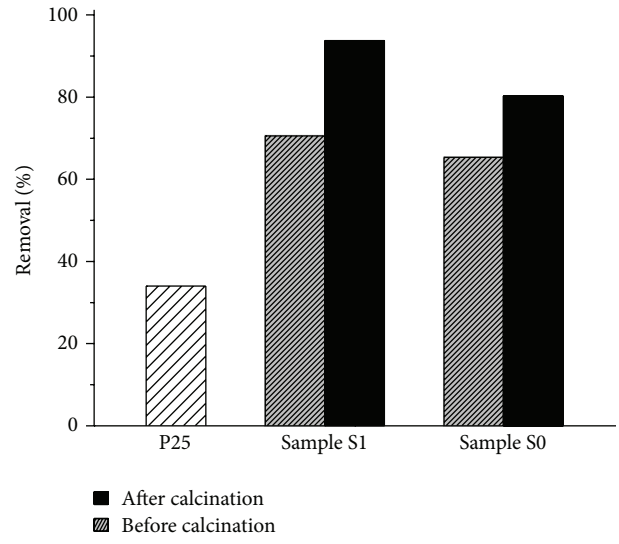

(a)

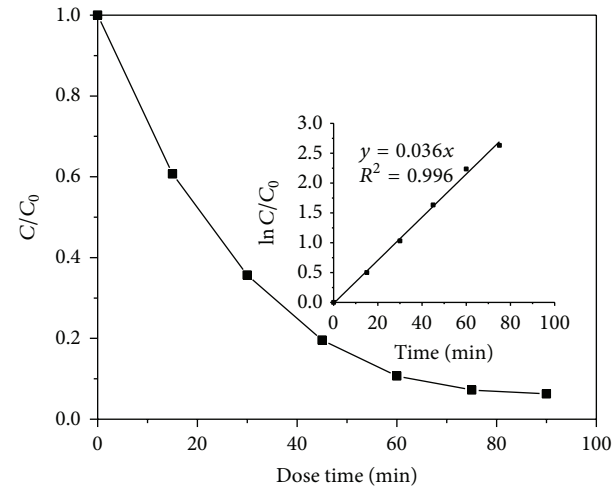

(b)

Figure 7: (a) Comparison of photocatalytic activity of P25 TiO_2 with as-synthesized TiO_2 films (S0 and S1) before and after heat treatment at 600°C. (b) Degradation curve and kinetics of bezafibrate degradation by {001} facets TiO_2 film.

were heat treated or not showed higher photocatalytic activity than P25, which indicates TiO_2 films with dominant {001} facets have higher activity. In addition, it can be observed that the addition of isopropanol in the hydrothermal mixture significantly affects the photocatalytic activity of as-synthesized samples. The photocatalytic decomposition of bezafibrate by TiO_2 films with dominant {001} facets follows pseudofirst order kinetics with a rate constant of 0.036 min^{-1} as shown in Figure 7(b). The sample S1 shows the highest activity with a rate constant of 0.0318 min^{-1} (removal ratio of 93.7% after calcination treatment at 600°C), nearly 2.6 times higher than that of P25 films coated on Ti-substrate. This can be attributed to the fact that the exposed percentage of {001} facets owned by sample S1 is higher than that of sample S0, as revealed from Raman spectra (Figure 4).

The role of fluorine in stabilizing {001} facets of anatase TiO_2 has been widely accepted. However, the influence of fluorine on the photocatalytic activity of anatase TiO_2 is still controversial. Some authors reported that it is good for enhancement of photocatalytic activity [16], while others have reported its negative impacts on photocatalytic activity [2]. As shown in Figure 7(a), after removal of surface-bonded fluoride ions via calcination treatment at 600°C, both samples S1 and S0 show better activity. The reason for its negative impact on fluorine element may be partly due to the strong binding between fluoride ions (F^-) and Ti^{4+} ions. In addition, the residual organic compounds on the surface of as-synthesized samples before calcination may also influence their photocatalytic activity. Figure 8 shows the diffuse reflectance UV-absorption spectrum of sample S1 before and after calcination. It can be seen that there is an obvious absorption tail at 400 nm before calcination which is probably due to the existence of colored organic compounds on the surface of TiO_2 films, while it almost disappears after calcination treatment at 600°C.

Photocatalytic stability over a large period of time is an important aspect of developing a suitable material for an industrial photocatalysis process. Figure 9 shows that more than 90% of bezafibrate was degraded within 120 min by sample S1, which was synthesized with addition of isopropanol into the hydrothermal solution, and its activity remained almost the same during the six cycles. However, sample S0, which was synthesized without addition of isopropanol and had spherical morphology, degraded 80.3% of bezafibrate in the first run within 120 min. Furthermore, its activity gradually decreased in the subsequent runs, and only 65% of bezafibrate degraded at the sixth run. The deterioration of photocatalytic activity of sample S0 may be due to the loose

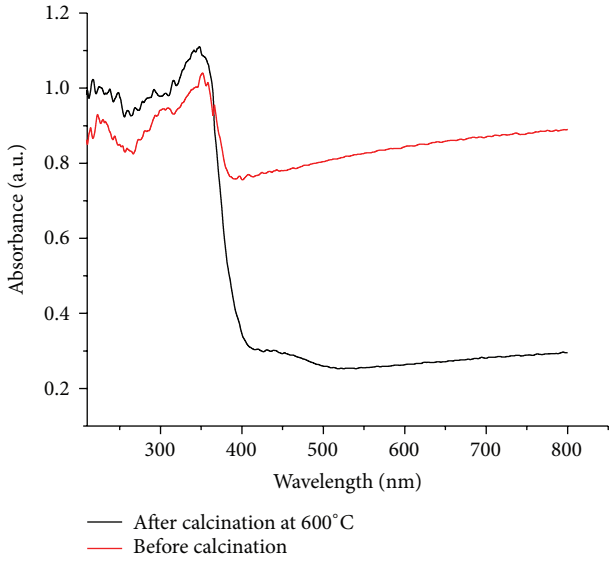

FIGURE 8: UV-Vis diffuse reflectance spectra of as-synthesized TiO_2 films before and after heat treatment at 600°C.

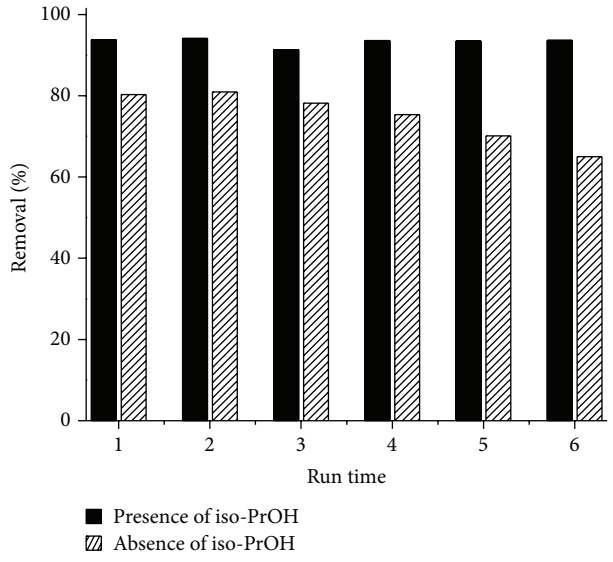

FIGURE 9: Photocatalytic stability of TiO_2 films synthesized with and without addition of isopropanol.

adherence of microspheres to the Ti-substrate, and the as-synthesized TiO_2 microsphere films more easily peel from the Ti substrate.

3.6. Degradation Intermediates and Pathway. It has been observed that during advanced oxidation processes (AOPs), including TiO_2 photocatalysis, various degradation intermediates can be generated. The exact identification of all the degradation products (DPs) present in the sample solution is a difficult task, as sometimes the concentrations at which they are generated are too low to be identified.

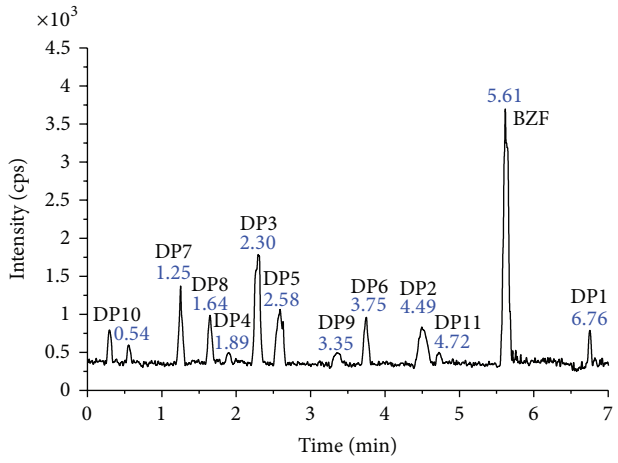

FIGURE 10: Total ion chromatogram (TIC) of bezafibrate sample after 90 min of UV-irradiation in the presence of {001} facets TiO_2 film (sample S1) showing the bezafibrate peak and its degradation intermediates.

Semipolar and polar degradation products were analyzed by UPLC-MS/MS with the electrospray ionization mode. Figure 10 shows the total ion-chromatogram (TIC) of bezafibrate solution after being photocatalytically treated for 90 min by sample S1. The detailed examination of all the peaks present in the chromatogram gives the identification of bezafibrate DPs on the basis of their accurate mass measurements and the information provided by the system software, which calculates the elemental composition and empirical formula, generating a list of best-match hits. All the identified products are eluted before bezafibrate, except one (DP1), involving the formation of smaller and more polar products as compared to the parent compound. Table 1 shows data related to degradation products including their calculated and observed masses, chemical formula, and structures.

Various degradation products identified with UPLC-MS/MS were the consequence of $^{\bullet}OH$ radical attack on the aromatic moiety. Since there are two benzene rings in the bezafibrate molecule, various hydroxylated intermediates were detected as summarized in Figure 11. There are two possibilities for the attack of $^{\bullet}OH$ radical, either hydroxylation on the 4-cholorobenzoyl ring or hydroxylation of the phenoxy moiety [38].

Since $^{\bullet}OH$ radical has strong electrophilic character, it will attack the carbon atoms with highest electron density, that is, the phenoxy ring. On the contrary, the chlorine containing ring has lower reactivity as compared to unchlorinated one due to the electron withdrawing effect of chlorine itself. So, on the basis of structural information of the target compound, $^{\bullet}OH$ radical preferably attacks at the phenoxy ring and the attack at 4-chlorobezoyl moiety may be the minor route.

The reaction product with MW of 343 (DP2) results from oxidative dechlorination of bezafibrate molecule by $^{\bullet}OH$ radical attack at the ipso-chloro position. Similarly, the product with MW of 275 (DP3) results from the attack of $^{\bullet}OH$ at phenoxy side of bezafibrate molecule, which further gives

Table 1: BZF derivatives produced during photocatalytic degradation by {001} facets TiO_2 film.

Number	Retention time (min)	Chemical structure	Formula	Observed m/z	Calculated m/z
DP1	6.76	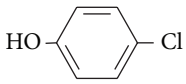	C_6H_5ClO	128.5568	128.5563
DP2	4.49	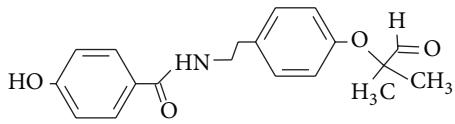	$C_{19}H_{21}NO_5$	343.3728	343.3737
DP3	2.30	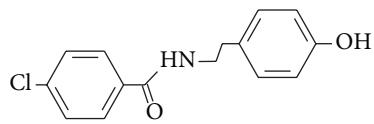	$C_{15}H_{14}ClNO_2$	275.73072	275.73016
DP4	1.89	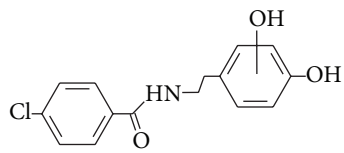	$C_{15}H_{14}ClNO_3$	291.7286	291.7296
DP5	2.58	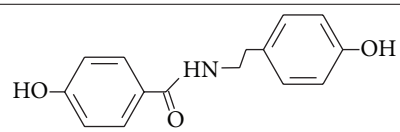	$C_{15}H_{15}NO_3$	257.2849	257.2845
DP6	3.75	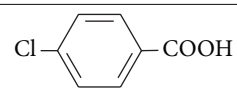	$C_7H_5ClO_2$	156.5660	156.5664
DP7	1.25	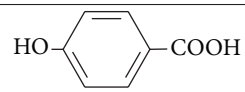	$C_7H_6O_3$	138.1215	138.1207
DP8	1.64	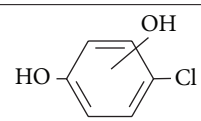	$C_6H_5ClO_2$	144.5561	144.5557
DP9	3.35	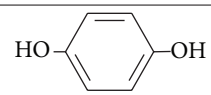	$C_6H_6O_2$	110.1114	110.1106
DP10	0.54	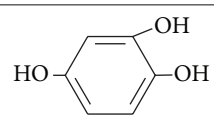	$C_6H_6O_3$	126.1100	126.1100
DP11	4.72	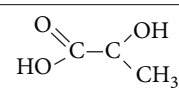	$C_3H_6O_3$	90.0779	90.0779

hydroxy-substituted products with MW of 291 (DP4), 257 (DP5), and 138 (DP7). Degradation product with MW of 157 (DP6) shows the formation of 4-chlorobenzoic acid, which further favors decarboxylation instead of hydroxylation of the aromatic ring resulting in the formation of 4-cholorphenol (DP1) via the photo-Kolbe reaction mechanism [39]. Further degradation of 4-chlorophenol results in the degradation products with MW of 144 (4-chlorocatechol, 4-chlororesorcinol, and hydroquinone) and then to hydroxyhydroquinone (DP10), which are in agreement with previous results [40]. Formation of lactic acid (DP11) shows that target compound can be converted to short chain carboxylic acids via the breaking of the aromatic ring.

4. Conclusions

A highly stable and reactive anatase TiO_2 film with dominant {001} facets can be synthesized by a simple hydrothermal technique in the presence of isopropanol. The percentage of exposed {001} facets increased from 48.2% to 57% with

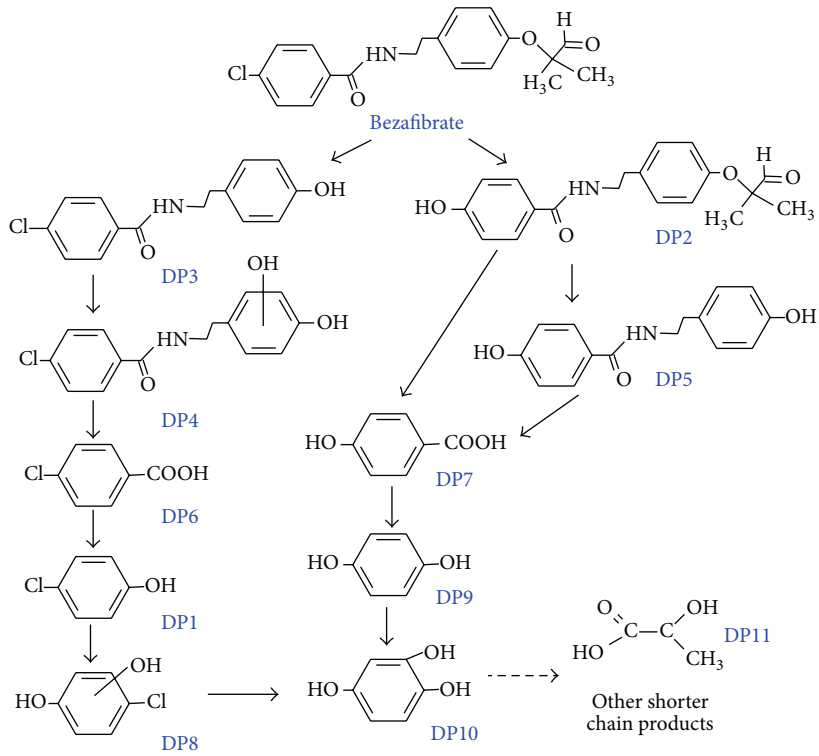

Figure 11: Photocatalytic degradation pathway for bezafibrate by {001} facets TiO_2 film.

addition of isopropanol in the hydrothermal solution. Furthermore, the surface morphology changed from nanosheet-assembled microspheres into irregular stack of truncated tetrahedrons, with the thickness decreasing from ~30 μm to <1 μm. As-synthesized TiO_2 films show excellent photocatalytic activity, far exceeding that of commercially available P25 TiO_2 due to exposure of high percentage of {001} facets. The addition of isopropanol into the hydrothermal solution also plays a crucial role in enhancing the stability of as-synthesized {001} facets TiO_2 film. Different degradation products were identified by UPLC-MS/MS as the consequence of $^{\bullet}OH$ radical attack on the aromatic moiety. The present study motivates us to further explore the role of alcohols in the synthesis of high energy {001} facets TiO_2 film for more promising applications.

Conflict of Interests

The authors declare that there is no conflict of interests regarding the publication of this paper.

Acknowledgments

This work was funded by the National Basic Research Program of China (2013CB632403), Science Fund for Creative Research Groups (21221004), and the Collaborative Innovation Center for Regional Environmental Quality. Murtaza Sayed is thankful to Higher Education Commission (HEC) of Pakistan for his Ph.D. grant to Tsinghua University, Beijing, China.

References

[1] D. Friedmann, C. Mendive, and D. Bahnemann, "TiO_2 for water treatment: parameters affecting the kinetics and mechanisms of photocatalysis," *Applied Catalysis B: Environmental*, vol. 99, no. 3-4, pp. 398–406, 2010.

[2] X. Han, Q. Kuang, M. Jin, Z. Xie, and L. Zheng, "Synthesis of titania nanosheets with a high percentage of exposed (001) facets and related photocatalytic properties," *Journal of the American Chemical Society*, vol. 131, no. 9, pp. 3152–3153, 2009.

[3] G. Liu, H. G. Yang, X. Wang et al., "Visible light responsive nitrogen doped anatase TiO_2 sheets with dominant {001} facets derived from TiN," *Journal of the American Chemical Society*, vol. 131, no. 36, pp. 12868–12869, 2009.

[4] M. Liu, L. Piao, W. Lu et al., "Flower-like TiO_2 nanostructures with exposed {001} facets: facile synthesis and enhanced photocatalysis," *Nanoscale*, vol. 2, no. 7, pp. 1115–1117, 2010.

[5] G. Wu, J. Wang, D. F. Thomas, and A. Chen, "Synthesis of F-doped flower-like TiO_2 nanostructures with high photoelectrochemical activity," *Langmuir*, vol. 24, no. 7, pp. 3503–3509, 2008.

[6] H. G. Yang, G. Liu, S. Z. Qiao et al., "Solvothermal synthesis and photoreactivity of anatase TiO_2 nanosheets with dominant {001} facets," *Journal of the American Chemical Society*, vol. 131, no. 11, pp. 4078–4083, 2009.

[7] H. G. Yang, C. H. Sun, S. Z. Qiao et al., "Anatase TiO_2 single crystals with a large percentage of reactive facets," *Nature*, vol. 453, no. 7195, pp. 638–641, 2008.

[8] J. Yu, L. Qi, and M. Jaroniec, "Hydrogen production by photocatalytic water splitting over Pt/TiO_2 nanosheets with exposed (001) facets," *Journal of Physical Chemistry C*, vol. 114, no. 30, pp. 13118–13125, 2010.

[9] Y. Alivov and Z. Y. Fan, "A method for fabrication of pyramid-shaped TiO_2 nanoparticles with a high {001} facet percentage," *Journal of Physical Chemistry C*, vol. 113, no. 30, pp. 12954–12957, 2009.

[10] S. Liu, J. Yu, and M. Jaroniec, "Tunable photocatalytic selectivity of hollow TiO_2 microspheres composed of anatase polyhedra with exposed {001} facets," *Journal of the American Chemical Society*, vol. 132, no. 34, pp. 11914–11916, 2010.

[11] J. Yu, J. Fan, and K. Lv, "Anatase TiO_2 nanosheets with exposed (001) facets: improved photoelectric conversion efficiency in dye-sensitized solar cells," *Nanoscale*, vol. 2, no. 10, pp. 2144–2149, 2010.

[12] J. S. Chen, Y. L. Tan, C. M. Li et al., "Constructing hierarchical spheres from large ultrathin anatase TiO_2 nanosheets with nearly 100% exposed (001) facets for fast reversible lithium storage," *Journal of the American Chemical Society*, vol. 132, no. 17, pp. 6124–6130, 2010.

[13] Y. Dai, C. M. Cobley, J. Zeng, Y. Sun, and Y. Xia, "Synthesis of anatase TiO_2 nanocrystals with exposed {001} facets," *Nano Letters*, vol. 9, no. 6, pp. 2455–2459, 2009.

[14] H. Ariga, T. Taniike, H. Morikawa et al., "Surface-mediated visible-light photo-oxidation on pure TiO_2(001)," *Journal of the American Chemical Society*, vol. 131, no. 41, pp. 14670–14672, 2009.

[15] D. Zhang, G. Li, X. Yang, and J. C. Yu, "A micrometer-size TiO_2 single-crystal photocatalyst with remarkable 80% level of reactive facets," *Chemical Communications*, no. 29, pp. 4381–4383, 2009.

[16] Q. Xiang, K. Lv, and J. Yu, "Pivotal role of fluorine in enhanced photocatalytic activity of anatase TiO_2 nanosheets with dominant (001) facets for the photocatalytic degradation of acetone in air," *Applied Catalysis B: Environmental*, vol. 96, no. 3-4, pp. 557–564, 2010.

[17] X. Wang, G. Liu, L. Wang, J. Pan, G. Q. M. Lu, and H.-M. Cheng, "TiO_2 films with oriented anatase {001} facets and their photoelectrochemical behavior as CdS nanoparticle sensitized photoanodes," *Journal of Materials Chemistry*, vol. 21, no. 3, pp. 869–873, 2011.

[18] H. Zhang, Y. Wang, P. Liu et al., "Anatase TiO_2 crystal facet growth: mechanistic role of hydrofluoric acid and photoelectrocatalytic activity," *ACS Applied Materials and Interfaces*, vol. 3, no. 7, pp. 2472–2478, 2011.

[19] J.-M. Wu and M.-L. Tang, "Hydrothermal growth of nanometer- to micrometer-size anatase single crystals with exposed (001) facets and their ability to assist photodegradation of rhodamine B in water," *Journal of Hazardous Materials*, vol. 190, no. 1-3, pp. 566–573, 2011.

[20] S. Zhu and H. Chen, "The fate and risk of selected pharmaceutical and personal care products in wastewater treatment plants and a pilot-scale multistage constructed wetland system," *Environmental Science and Pollution Research*, vol. 21, no. 2, pp. 1466–1479, 2014.

[21] C. G. Daughton and T. A. Ternes, "Pharmaceuticals and personal care products in the environment: agents of subtle change?" *Environmental Health Perspectives*, vol. 107, no. 6, pp. 907–938, 1999.

[22] T. A. Ternes, "Occurrence of drugs in German sewage treatment plants and rivers," *Water Research*, vol. 32, no. 11, pp. 3245–3260, 1998.

[23] D. Calamari, E. Zuccato, S. Castiglioni, R. Bagnati, and R. Fanelli, "Strategic survey of therapeutic drugs in the rivers Po and lambro in Northern Italy," *Environmental Science and Technology*, vol. 37, no. 7, pp. 1241–1248, 2003.

[24] A. G. Trovó, S. A. S. Melo, and R. F. P. Nogueira, "Photodegradation of the pharmaceuticals amoxicillin, bezafibrate and paracetamol by the photo-Fenton process—application to sewage treatment plant effluent," *Journal of Photochemistry and Photobiology A: Chemistry*, vol. 198, no. 2-3, pp. 215–220, 2008.

[25] M. Cermola, M. DellaGreca, M. R. Iesce et al., "Phototransformation of fibrate drugs in aqueous media," *Environmental Chemistry Letters*, vol. 3, no. 1, pp. 43–47, 2005.

[26] H. Yuan, Y. Zhang, and X. Zhou, "Degradation of bezafibrate with UV/H_2O_2 in surface water and wastewater treatment plant effluent," *Clean—Soil, Air, Water*, vol. 40, no. 3, pp. 239–245, 2012.

[27] J. Yu, W. Wang, B. Cheng, and B.-L. Su, "Enhancement of photocatalytic activity of mesporous TiO_2 powders by hydrothermal surface fluorination treatment," *Journal of Physical Chemistry C*, vol. 113, no. 16, pp. 6743–6750, 2009.

[28] X. Wang, H. He, Y. Chen, J. Zhao, and X. Zhang, "Anatase TiO_2 hollow microspheres with exposed {001} facets: facile synthesis and enhanced photocatalysis," *Applied Surface Science*, vol. 258, no. 15, pp. 5863–5868, 2012.

[29] S.-Y. Yang, Y.-Y. Chen, J.-G. Zheng, and Y.-J. Cui, "Enhanced photocatalytic activity of TiO_2 by surface fluorination in degradation of organic cationic compound," *Journal of Environmental Sciences*, vol. 19, no. 1, pp. 86–89, 2007.

[30] Z.-T. Liu, X. Li, Z.-W. Liu, and J. Lu, "Synthesis and catalytic behaviors of cobalt nanocrystals with special morphologies," *Powder Technology*, vol. 189, no. 3, pp. 514–519, 2009.

[31] X.-M. Song, J.-M. Wu, M.-Z. Tang, B. Qi, and M. Yan, "Enhanced photoelectrochemical response of a composite titania thin film with single-crystalline rutile nanorods embedded in anatase aggregates," *Journal of Physical Chemistry C*, vol. 112, no. 49, pp. 19484–19492, 2008.

[32] X.-M. Song, J.-M. Wu, and M. Yan, "Distinct visible-light response of composite films with CdS electrodeposited on TiO_2 nanorod and nanotube arrays," *Electrochemistry Communications*, vol. 11, no. 11, pp. 2203–2206, 2009.

[33] F. Tian, Y. Zhang, J. Zhang, and C. Pan, "Raman spectroscopy: a new approach to measure the percentage of anatase TiO_2 exposed (001) facets," *Journal of Physical Chemistry C*, vol. 116, no. 13, pp. 7515–7519, 2012.

[34] T. Ohsaka, F. Izumi, and Y. Fujiki, "Raman spectrum of anatase, TiO_2," *Journal of Raman Spectroscopy*, vol. 7, no. 6, pp. 321–324, 1978.

[35] D. Bersani, P. P. Lottici, and X.-Z. Ding, "Phonon confinement effects in the Raman scattering by TiO_2 nanocrystals," *Applied Physics Letters*, vol. 72, no. 1, pp. 73–75, 1998.

[36] X. H. Yang, Z. Li, G. Liu et al., "Ultra-thin anatase TiO_2 nanosheets dominated with {001} facets: thickness-controlled synthesis, growth mechanism and water-splitting properties," *CrystEngComm*, vol. 13, no. 5, pp. 1378–1383, 2011.

[37] J. C. Yu, J. Yu, W. Ho, Z. Jiang, and L. Zhang, "Effects of F-doping on the photocatalytic activity and microstructures of nanocrystalline TiO_2 powders," *Chemistry of Materials*, vol. 14, no. 9, pp. 3808–3816, 2002.

[38] D. A. Lambropoulou, M. D. Hernando, I. K. Konstantinou et al., "Identification of photocatalytic degradation products of bezafibrate in TiO_2 aqueous suspensions by liquid and gas chromatography," *Journal of Chromatography A*, vol. 1183, no. 1-2, pp. 38–48, 2008.

[39] H. Tahiri, Y. A. Ichou, and J.-M. Herrmann, "Photocatalytic degration of chlorobenzoic isomers in auqeous suspensions of neat and modified titania," *Journal of Photochemistry and Photobiology A: Chemistry*, vol. 114, no. 3, pp. 219–226, 1998.

[40] G. Al-Sayyed, J.-C. D'Oliveira, and P. Pichat, "Semiconductor-sensitized photodegradation of 4-chlorophenol in water," *Journal of Photochemistry and Photobiology A: Chemistry*, vol. 58, no. 1, pp. 99–114, 1991.